

# QUALITY MEASUREMENTS OF 3D LIGHT-FIELD DISPLAYS

Péter Tamás Kovács<sup>1,2</sup>, Atanas Boev<sup>2</sup>, Robert Bregović<sup>2</sup>, Atanas Gotchev<sup>2</sup>

<sup>1</sup>Holografika, Budapest, Hungary

<sup>2</sup>Department of Signal Processing, Tampere University of Technology, Tampere, Finland

## ABSTRACT

We present methods to measure the spatial, angular and depth resolution of LF displays using off-the-shelf equipment and performing a subjective experiment. The spatial resolution is measured in circles per degree and the challenge is to display and quantify sinusoidal patterns with varying spatial frequencies on displays, which in general do not exhibit regular or pixel-like structure. Being specific for 3D displays, the angular resolution represents the number of unique directions that can be emitted from a point, and measured in circles per degree. The paper presents the experimental setup and discusses the results. The depth resolution shows the minimum distinguishable depth that can be reproduced by the display used, and is estimated by a subjective experiment.

## 1. INTRODUCTION

3D displays are expected to reconstruct 3D visual scenes with certain level of realism relying on various 3D visual cues. Auto-stereoscopic (AS) and multi-view (MV) displays generate a discrete set of *views* (two or more) forming stereo-pairs thus providing binocular cues without the need of wearing 3D glasses [1]. Observers are supposed to find the proper viewpoint (sweet spot) where the views from a stereo pair are best visible by the corresponding eyes. AS displays do not provide head parallax and MV displays provide a very limited one resulting from the limited set of discrete views available. This is usually accompanied by the effect of transition (jump) between those views and known as *image flipping*.

The next generation of 3D displays, denoted as light-field (LF) displays aim at providing a continuous head parallax experience over a wide viewing zone with no use of glasses. In general, this requires a departure from the ‘discrete view’ formalism. Instead, a certain continuous reconstruction of the light field emanated or reflected from the 3D visual scene is targeted. Correspondingly, the scene is represented by a discrete set of light rays, which serve as generators for the subsequent process of continuous light field reconstruction.

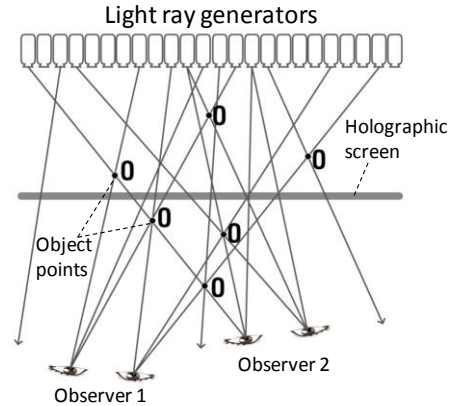


Figure 1: Light-field display architecture

Technologically, this two-stage process (scene representation and scene reconstruction) can be implemented by using an array of projection modules emitting light rays toward a custom-made LF reconstruction surface (screen). The latter makes the optical transformation that composes rays into a continuous LF [9].

With proper design of the LF display, light rays leaving the screen spread in multiple directions, as if they were emitted from points of 3D objects at fixed spatial locations. This gives the illusion of points appearing either behind the screen, on the screen, or floating in front of it, achieving an effect similar to holograms, as illustrated in Figure 1. Therefore, the LF reconstruction screen is sometimes denoted as a *holographic* screen.

With the emergence of LF displays, the issue of their quality and its characterization becomes of primary importance. For 2D displays, display quality is directly characterized by their spatial resolution and observation angle, which quantification and measurement are standardized [4] and therefore, easily available to and interpretable by the end users. Manufacturers of 3D displays do not follow a single metric. Instead, they either describe display quality using 2D-related parameters or provide no such information at all. For example, the visualization capabilities of a 3D display are given in terms of the underlying TFT matrix resolution and the number of unique views [16].

Most previous work related to characterization of 3D displays is focused on stereoscopic and multi-view (MV) displays. The work presented in [2] provides an approach to model multi-view displays in the frequency domain using test patterns with various density and orientation. However, the work assumes a MV display with a sub-pixel interleaving topology – something that LF displays do not have. The approach presented in [3] targets MV displays as well. This method is based on proprietary measurement equipment with Fourier optics, and due to the small size of the instrument, the applicability for large-scale (non-desktop) LF displays is limited. Moreover, it cannot be used for front-projected LF displays as the head would block the light path. The Information Display Measurement Standard [4] contains measurement methods for spatial and angular resolution (chapters 17.5.4 and 17.5.1 in [4]). The method described as angular resolution measurement relies on counting local maxima of a test pattern, but also assumes that the display can show two-view test patterns specifically targeting adjacent views, which is not directly applicable for LF displays. The method also assumes that the pixel size of the display is known in advance, which is not applicable for an LF display. The authors of [5] describe another proprietary measurement instrument, but the measurement assumes that the display is view-based, which does not apply for typical LF displays. We are not aware of a method that can measure the spatial and angular resolution of LF display with no discrete pixel structure.

In this work, we identify three parameters with direct influence on the perceptual quality of a LF display. *Spatial resolution* and *angular resolution*, both quantified in circles per degree (CPD) can be measured by off-the-shelf equipment. The minimum perceivable depth at the screen level, referred to as *perceptual depth resolution* is estimated by a subjective experiment. We specifically experiment with displays produced using HoloVizio technology [8] however the methodology can be easily adapted to other types of LF displays.

## 2. SPATIAL RESOLUTION

### 2.1. Background

The 2D spatial resolution of a LF display cannot be directly measured in terms of horizontal and vertical pixel count. This is due to the specific interaction between the discrete set of rays coming from projectors and the continuous LF reconstruction screen. For the proper generation of 3D effect, rays coming from different projectors might not form a regular structure. Correspondingly, the group of rays visible from a given direction do not appear as “pixels” on a rectangular grid [2].

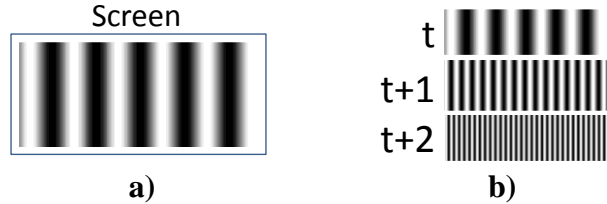


**Figure 2: a) Sinusoidal pattern for spatial resolution measurement; b) Sinusoids of increasing frequency used for the spatial resolution measurement**

Therefore, in our approach, the spatial resolution is quantified through the display capability to produce fine details with a given spatial orientation. In practice, this means measuring the display’s capability to reliably reproduce sinusoidal patterns in various directions.

One way to measure the 2D resolution would be to have an objective metric that analyses the contrast ratio of a sinusoidal pattern visualized on the screen. By measuring the contrast ratios of patterns with various density and orientations, one can find the threshold in each case, thereby determining the maximal resolution for the direction in question. However, rendering a sinusoidal pattern onto a non-rectangular grid produces imaging and aliasing distortions, which manifest themselves as Moiré patterns [7]. Therefore, measuring the contrast alone is not enough to assess how these distortions affect the image.

A more perceptually correct way to measure the 2D resolution would be to measure the so-called “pass-band” of the display [7]. In essence, pass-band measurement consists of a series of pass/fail tests, where each test analyses the distortions introduced by the display on a given test pattern. One starts with a test pattern with a given frequency and orientation, visualizes it on the screen, photographs it and analyses the output in the frequency domain. If the input (desired) frequency is still the dominant frequency on the output (distorted) image, the frequency of the pattern under test is considered to belong to the pass-band of the display. By repeating the pass/fail test for multiple test patterns, one can discover a large set of “passing” input frequencies. Union of all those frequencies is the pass-band of the display [7].

### 2.2. Experimental setup

Spatial resolution measurement involves showing sinusoidal black and white patterns of increasing frequency on the screen, taking photos of the resulting images and analyzing these photos in the frequency domain to determine the limits of visibility. The full-screen patterns projected on the screen show a sinusoidal change in intensity in one direction, but constant intensity in the orthogonal direction. The pattern used to measure horizontal resolution is shown in Figure 2a.

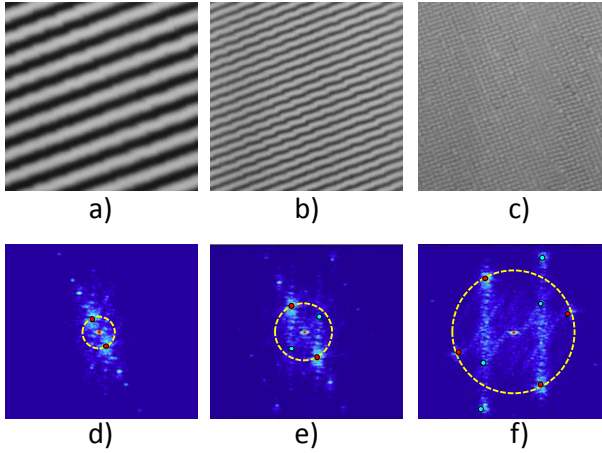


**Figure 3: Gratings with slant 22.5 degrees, tested for frequency dominance: a) grating with negligible distortions, b) grating with visible distortions, c) grating with ambiguous dominant frequency, d)-e) frequency analysis of the three gratings**

The frequency of the sinusoidal pattern is then increased and with every increment a new photo is taken (see Figure 2b). This procedure is then repeated with other measured directions (8 in our experiments), and a sequence of photos is taken starting from low frequency, with the same increments.

The measured directions of the test patterns are  $0^\circ$ ,  $22.5^\circ$ ,  $-22.5^\circ$ ,  $45^\circ$ ,  $-45^\circ$ ,  $67.5^\circ$ ,  $-67.5^\circ$  and  $90^\circ$ . These provide a good estimation of the display's pass-band.

As the LF image is comprised of a set of light rays originating from various sources, sampling and visualizing this pattern is not trivial. For this purpose, we have developed a pattern generator software that enumerates all the light rays emitted by the display. By knowing where the light rays originate from and where they cross the screen's surface, the intensity of the specific light ray is determined, much like a procedural texture. The direction and frequency of the pattern can be changed interactively or automatically. In automatic operation mode the software is also able to control a DSLR camera attached to the computer controlling the display, which takes photos corresponding to each pattern. The camera in this experiment is on a static stand, and is positioned so that it is pointing to the center of the screen and is in line with the screen center both horizontally and vertically. Camera settings shutter speed is set up so that the shutter speed is longer than the double of the refresh rate used by the display. The resolution of the camera is order of magnitude higher than what is needed for sampling of the grating with the highest frequency. The ISO and aperture are set so that is set so that the white and black intensities do not over saturate the camera, but still exploit most of its dynamic range.

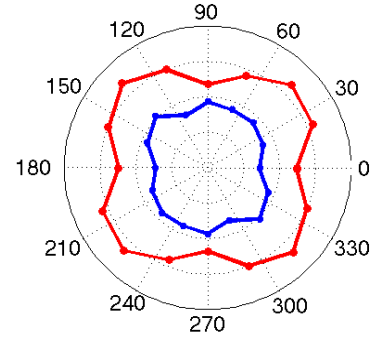


**Figure 4: Sample polar plot of resolution limits in different directions on the screen**

The resolution of the camera is set so that it oversamples the test pattern with the highest frequency. The camera is linearized as described in [15].

### 2.3. Analysis

Signals with measured frequencies lower than the frequency of the generated signal (i.e. aliased frequencies) are classified as distortions [7]. We consider distortion with amplitude 5% of the original (input) signal to be barely visible, and distortion with amplitude of 20% as unacceptable.

In other words, distortion with amplitude between 5% and 20% will produce visible distortions, but the original signal is still recognizable; distortion with amplitude greater than 20% results in perceptual loss (masking) of the original signal [7].

We start the analysis with cropping the acquired photos - we keep only the part depicting the visualized test pattern. Each cropped image is then windowed and a 2D FFT is executed on it. In the spectrum we can identify the peak that corresponds to the original frequency, and other peaks, which are created by display distortions. Next, we create the so-called unit circle around the point of origin, with a radius equal to the distance between the original peak and the point of origin. We search for peaks inside the unit circle. If the amplitude of such peaks is between 5% and 20% of the amplitude of the original one, we deem the patch to exhibit visible distortions. If the amplitude of the extra peaks is higher than 20% of the amplitude of the original one, then the dominant frequency is lost, and we deem the patch to have intolerable distortions.

An example of sinusoidal gratings under test is shown in Figure 3 a)-c) and frequency domain representations of these gratings can be seen in Figure 3 d)-f). The unit circle is plotted with yellow dashed line. The first grating exhibits minor distortions, and all peaks in the unit circle have negligible amplitude. The second grating has visible distortions, which appear as minor (5-20%) peaks inside the unit circle. In the third grating the dominant frequency is lost, and this can be detected by finding large peaks

inside of the unit circle. Such analysis is repeated for gratings with increasing density slanted in all preselected directions. The gathered data allows one to estimate the resolution of the display for details with different orientation in terms of cycles-per-degree (CPD). The resolution in a certain direction is estimated from the threshold for lines in the orthogonal direction – e.g. the horizontal resolution is estimated using a grating with vertical lines. Two sets of resolutions can be derived. One is what we call *distortion-free resolution*, i.e. the amount of cycles per degree the display can reproduce in a given direction, without introducing visible distortions. The other is *peak resolution*, which characterizes the maximum amount of CPD for which the introduced distortions do not mask the original signal. An example of these two resolutions derived for a LF display for different directions is given in Figure 4 – the blue line marks distortion-free resolution in CPD, while the red one marks the peak resolution. The data points in the figure indicate display resolution in a given direction.

### 3. ANGULAR RESOLUTION

#### 3.1. Background

The angular resolution of a multi-view display can be directly derived from the geometrical properties of the display, that is, it is related to the number of views the display can generate throughout its Field Of View (FOV). It can be calculated by dividing the FOV of the display with the number of views, or alternatively, it can be measured, for example, by the approach proposed in [2].

In the case of LF displays, the concept of views is abandoned. Instead, the angular resolution is determined by the minimal angle of change that rays can reproduce with respect to a single point on the screen. In a simplified form, the minimal angle that an ideal display should reproduce can be estimated based on the properties of the human visual system, as [13]

$$\theta_{min}^{(ideal)} = \tan^{-1} \frac{d_p}{D} \quad (1)$$

where  $d_p$  is the pupil diameter,  $D$  is distance to the screen (more precisely to the visualized point under consideration) and  $\theta_{min}$  is the minimum angle between two rays originating from a single point that the eye can discriminate. Having smaller angular resolution limits the capabilities of the display, i.e. proper continuous-like parallax is limited to objects closer to the screen level. By knowing the angular resolution of an LF display, it is possible to prepare the content for the display (e.g. keeping the depth of the scene inside depth budget) that will result in higher visual quality.

As discussed earlier, due to different specifications provided by display manufacturers as well as the fact that rays might not originate from the same point on the

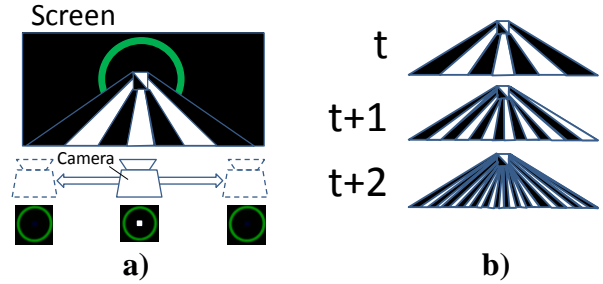


**Figure 5: a) Angular resolution test pattern, as seen by the camera from various angles. b) Angular resolution test patterns with increased frequency**

surface of the screen, it is not straightforward to evaluate the angular resolution based on that data. We are not aware of a systematical approach to measure the angular resolution of an LF display. Therefore, in the following section we describe an experimental setup for measuring the angular resolution. Similar principle as in the case of the spatial resolution measurement described in Section 2 is applied. First, a set of signals is generated that change the pixel intensity with observation angle, and then, second, the highest amount of change is evaluated for which these changes can be reliably detected by an observer. These changes are then related to the angular resolution.

#### 3.2. Experimental setup

Angular resolution measurement consists of showing a pattern that has a different appearance when viewed under different angles, that is, in this measurement, the direction selective light emission property of the 3D display is evaluated. We project a rectangular area that appears white from some viewing angles, and appears black from other angles. This black / white transition is repeated over the FOV of the display. A camera moving in front of the screen, pointing at the rectangle will see one or more white-to-black and black-to-white transitions during its travel (see Figure 5a). The duty cycle of black and white areas is always 50%, thus they appear to have the same size. Using a camera that moves parallel to the screen from one end of the display's FOV to the other end, a video is recorded. This video shows the intensity transitions of the measured spot as the screen is observed from various angles. The measurement spot is surrounded by a circle of solid green color that can be tracked in the recorded video. The angle between the observation direction where the measured spot is seen white and the direction it is seen black, is initially chosen to be large (e.g. two transitions over the whole FOV). Then the distance is gradually decreased, thus increasing the angular frequency of the pattern in subsequent iterations (see Figure 5b). Camera settings are as in the spatial resolution measurement.

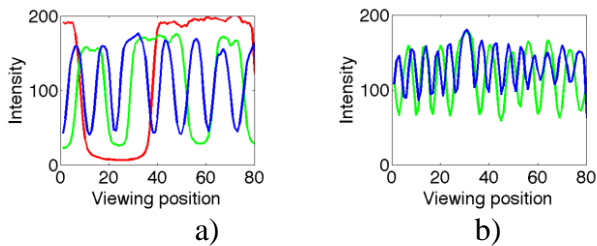


**Figure 6: a) Intensity of the measured spot with test patterns of increasing frequency ( $f_{\text{red}} < f_{\text{green}} < f_{\text{blue}}$ ) b) Decreased dynamic range for higher frequencies**

### 3.3. Analysis

From the video recordings, frames are extracted. On each frame, the center of the green marker circle is located giving the position of the measured spot. The intensity of the measured spot changes from low to high and high to low in successive frames (change in observation angle is related to the camera movement). This is shown in Figure 6a. In this figure we can also see the increased rate of transitions with patterns of increased frequency. As we proceed to higher frequency test patterns, the dynamic range between blacks and whites is decreasing (see Figure 6b and Figure 7a). We define the 2D dynamic range of the display to be difference between the black and white levels when a 2D image is shown. In that case, the dynamic range of different angular frequencies can be expressed proportionally to the 2D dynamic range, as shown in Figure 7b. Finally, we find the threshold where the angular dynamic range drops below 20% of the 2D dynamic range. We define the angular resolution of the display  $\theta_{\text{min}}$  to be equal to that threshold.

## 4. PERCEIVED DEPTH RESOLUTION

### 4.1. Background

As a result from the continuous head parallax an LF display can provide, the recreated scene appears visually as a 3D volume seen from various angles. Apart from planar (2D, or x-y) resolution, one might be interested also in the resolution in z-direction, i.e. what is the minimum depth difference that can be reliably reproduced by the display. The available parallax is characterized directly by the spatial resolution and the display FoV. The angular resolution naturally specifies how much one can move objects of size of one spatial element in front of the display before starting losing spatial resolution. Thus, the minimum perceivable depth is a function of the spatial and the angular resolution, but cannot be fully characterized by those since there are subjective factors such as motion speed, memory and temporal masking along with other degradation factors, such as inter-perspective crosstalk and

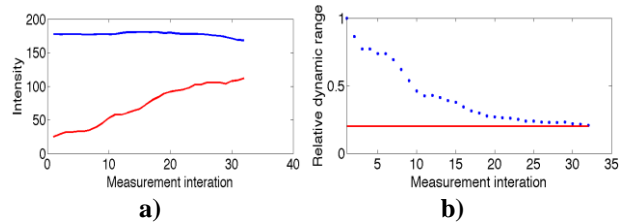


**Figure 7: a) Highest and lowest intensities as observed with successive angular resolution test patterns (blue: highest intensity, green: lowest intensity) b) Relative dynamic range**

texture blur, which influence the ability of the observers to discriminate depth layers [6][9]. Besides, human vision is less sensitive to depth variations than to spatial variations of the same magnitude [12].

Usually, studies on stereoscopic perception use random dot stereograms to assess the thresholds in perceiving depth [10][12]. Experiments involving sinusoidal depth plane discrimination have been used to study disparity [10] or motion parallax [11] thresholds. In this work, we aim at finding the minimal step in z-direction that can be observed on a particular LF display, providing certain level of continuous parallax, by means of a direct subjective experiment.

### 4.2. Experimental setup

In this measurement we show a 3D object with a sinusoidal depth grating having a random dot texture. The grating is a surface with sinusoidal depth profile, as shown in Figure 8a and Figure 8b. The texture shows smooth circles of various sizes. It is projected orthogonally onto the surface, so that for an observer staying in front of the display the texture has no projective distortions and bears no pictorial depth cues (see Figure 8c). The grating is visualized as being parallel to the screen, and is scaled so that its borders appear outside of the screen area. A grating with zero amplitude appears as a flat surface parallel to the screen, while a grating with depth variations appears as sinusoidal surface changing alternatively towards and away from the observer. The only depth cues of the scene are the interocular and head parallax created by the LF display.

The experiment uses custom software that allows the density and the amplitude of the grating to be changed interactively. The experiment starts by showing a low-density sinusoidal grating with zero amplitude. The test subject is encouraged to move around and observe the grating from different perspectives, and is asked to distinguish whether the visualized grating is flat or grooved.

The amplitude of the grating is increased by 10% at a time, till the observer notices the depth changes of the grating. It should be noted, that the threshold sensitivity of

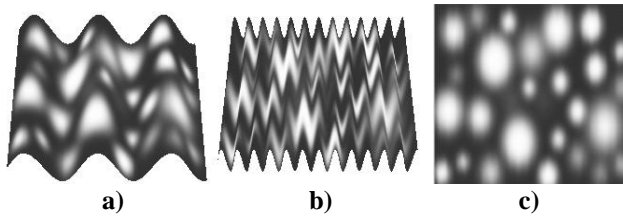


**Figure 8: Sinusoidal depth gratings: a) low density grating, b) high density grating, c) orthogonal observation of the high density grating**

the human vision to sinusoidal gratings varies with grating density [12]. We have selected planar frequencies in the range between 0.5 and 4 CPD, where the human vision has constant sensitivity to depth variations.

### 4.3 Analysis

The experiment has been performed with three volunteers, and using three grating frequencies. The perceptual thresholds for depth variations were recorded in terms of absolute distance values, as provided to the rendering engine. After the experiments, these were converted to relative values, relative to the total depth range provided by the display. The results are shown in Figure 9. Apparently, even though high angular frequency is needed for the display to provide continuous head parallax, much lower depth resolution would be sufficient for acceptable 3D representation of 3D data.

## 5. CONCLUSIONS

We have presented methods for measuring three characteristic parameters of 3D LF displays – namely spatial, angular and perceived depth resolution. The methods are suitable for LF displays, which do not have discrete pixels. Spatial resolution measurement is fully automatic, while the angular resolution measurement requires moving the camera. The proposed methods provide valuable information about the visualization capabilities of a given LF display, which can be utilized in capturing, compressing and visualizing of LF data.

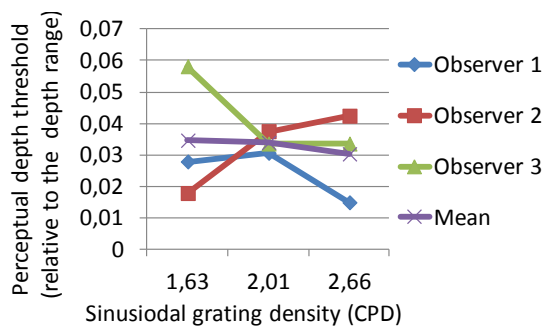


**Figure 9: Perceived depth resolution of the display**

## 6. ACKNOWLEDGEMENTS

The research leading to these results has received funding from the PROLIGHT-IAPP Marie Curie Action of the People programme of the European Union's Seventh Framework Programme, REA grant agreement 32449.

## 7. REFERENCES

- [1] 3D@Home Consortium and International 3D Society, "3D Display Technology Matrix- April 2012", [http://www.3dathome.org/images/Tech\\_Matrix\\_120329.html](http://www.3dathome.org/images/Tech_Matrix_120329.html), retrieved 23.10.2013
- [2] A. Boev, R. Bregovic, and A. Gotchev, "Measuring and modeling per-element angular visibility in multi-view displays," *J. of the Society for Information Display*, 18: 686–697. 2010, doi: 10.1889/JSID18.9.686
- [3] P. Boher, T. Leroux, T. Bignon, et al., "A new way to characterize autostereoscopic 3D displays using Fourier optics instrument," *Proc. SPIE 7237, Stereoscopic Displays and Applications XX*, 72370Z, February 17, 2009
- [4] The International Display Measurement Standard v1.03, The Society for Information Display, 2012
- [5] R. Rykowski, J. Lee, "Novel Technology for View Angle Performance Measurement," *IMID 2008*, Ilsan, Korea, 2008
- [6] F. Kooi, A. Toet, "Visual comfort of binocular and 3D displays", *Displays* 25 (2-3) (2004) 99–108. ISSN:0141-9382, doi:10.1016/j.displa.2004.07.004
- [7] A. Boev, R. Bregović, and A. Gotchev, "Visual-quality evaluation methodology for multiview displays," *Displays*, vol. 33, 2012, pp. 103-112, doi:10.1016/j.displa.2012.01.002
- [8] T. Balogh, "The HoloVizio system," *Proc. SPIE 6055, Stereoscopic Displays and Virtual Reality Systems XIII*, 60550U (January 27, 2006); doi:10.1117/12.650907
- [9] P.J.H. Seuntiëns, L.M.J. Meesters, W.A. IJsselsteijn, "Perceptual attributes of crosstalk in 3D images", *Displays*, Volume 26, Issues 4-5, October 2005, Pages 177-183, ISSN 0141-9382, 10.1016/j.displa.2005.06.005
- [10] M. Nawrot, "Depth from motion parallax scales with eye movement gain" *Journal of Vision* December 18, 2003
- [11] H. Ujike, H. Ono, "Depth thresholds of motion parallax as a function of head movement velocity", *J. of Vision Res.* 2001 Oct;41(22):2835-43.
- [12] D. Kane, P. Guan, M. Banks (in press). "The limits of human stereopsis in space and time". *Journal of Neuroscience*. Manuscript submitted for publication.
- [13] S. A. Benton and V. M. Bove Jr. *Holographic Imaging*, John Wiley and Sons, New Jersey, 2008.
- [14] S. Pastoor, "3D displays", in (Schreer, Kauff, Sikora, eds.) *3D Video Communication*, Wiley, 2005.
- [15] P. Debevec, J. Malik, "Recovering High Dynamic Range Radiance Maps from Photographs," in *Proc. ACM SIGGRAPH*, 1997
- [16] A. Schmidt and A. Grasnick, "Multi-viewpoint autostereoscopic displays from 4D-vision", in *Proc. SPIE Photonics West 2002: Electronic Imaging*, vol. 4660, pp. 212-221, 20023D